*International Journal of Latest Engineering Research and Applications (IJLERA) ISSN: 2455-7137*

*Volume – 02, Issue – 09, September – 2017, PP – 06-12*

# Passive Islanding Detection Technique for Grid-Connected Photovoltaic System in Time domain analysis

D. Devi Vara Prasad[1], B. Pangedaiah[2]

[1](EEE,PG Student, LBRCE/ JNTUK,INDIA)

[2](EEE,Sr.Asst Professor,LBRCE/ JNTUK, INDIA)

**Abstract:** Oneof the main challenges of integrating distributed generation into the power grid is islanding, which occurs when a part of the electrical power system is disconnected from the rest of the grid and is still energized by a DG unit. If islanding is not quickly detected, it can present serious safety and hazardous conditions. Conventional passive detection techniques used today are entirely dependent on the parameters of the power system, which under certain operating conditions may fail to detect islanding. In this paper, a passive islanding detection technique for grid-connected photovoltaic-based inverters is presented. The proposed technique utilizes the converter-induced ripples in the instantaneous voltage amplitude at the point of common coupling to detect islanding. The performance of this technique was extensively tested and quantified under a wide range of operating conditions. The results are presented in this paper using Matlab/simulink).

**Keywords:** Anti-islanding, distributed generation, passive islanding detection, smart grid, spectral analysis.

## I. INTRODUCTION

When the distribution network is disconnected from the grid, the first step would be to detect the islanding phenomenon. This requires an efficient islanding detection technique to detect the islanding event in order to operate or disconnect the DG. This is very important, as the failure to accurately detect islanding may result in the failure of the whole distribution network. Two factors are important in islanding detection, which are time and accuracy for each type of DG. Up to now, several remote, passive, active and hybrid islanding detection techniques have been proposed. However, each technique has its merits and demerits. Hence, the research interest shifts towards the application of computational intelligence-based techniques for islanding detection. The computational intelligence based techniques, due to their robustness and ability to easily deal with complex system, may be suitable for islanding detection of DG. This paper reviews the ability of these techniques in accurate and fast islanding detection.[1]

Islanding detection technique commonly uses frequency, voltage, active power, and reactive power parameters as a mean to detect the islanding event. The type of loads, affects all of these parameters which in turn affect the performance of islanding detection technique, as well as their non-detection zones. Several researchers have conducted the research to observe the effects of different types of loads (static load, dynamic load and composite load) on the performance of islanding detection technique. Static load model represents the active and reactive power of the load as functions of voltage and frequency. Static load models can be further divided into three types, namely constant power, constant current, and constant impedance loads. Dynamic load models represent the induction motors loads, whereas composite loads combine both static and dynamic type of loads to analyze their effect on distribution system.

Generally, there are mainly three types of islanding detection methods including communication-based, passive, and active methods. Active methods not resident in the inverter work similarly to the previous ones, but the action is taken on the grid side of the PCC. Communications-based methods involve a transmission of data between the inverter and the grid systems, and the data is used by the PV system to determine when to cease or continue operation[2].Though communication-based methods do no harm the power quality of the power system with the negligible non detection zone (NDZ), the cost is much higher than the other two types of methods and the operations are more complex as well. Therefore, passive and active methods have been well developed so far. Over/under frequency protection (OFP/UFP), over/under voltage protection (OVP/UVP), and phase jump detection are the most widely used passive islanding detection methods, which determine the islanding condition by measuring the PCC voltage and the current from the DG In power systems, under normal operating conditions, the amplitude of the PCC voltage is typically constant due to the stabilizing effect of the grid.[3] However, during islanding, the absence of the grid stabilizing effect may cause the amplitude of the signal to undergo sudden and sustained fluctuations which can be used to detect islanding. In this paper, a computationally efficient passive islanding detection technique for DG grid-connected PV systems is presented. The proposed technique is based on monitoring the time domain spectral content of the ripple in the PCC

 2017 IJLERA – All Right Reserved 

voltage that can be easily implemented in the inverter circuitry. Islanding is detected whenever the ripple spectral content exceeds a preset threshold level for a certain period of time. This technique does not have NDZ limitations and is able to detect islanding even in zero power mismatches where other passive techniques fail to detect. Moreover, the proposed technique detects islanding within 300 ms and is independent of the DG system size and parameters.

### 1.1. INVERTER-BASED DISTRIBUTED GENERATION MODEL

In a typical grid-connected PV system, the energy collected by the solar array is directed to the utility side through a series of electrical devices that condition and convert the DC signal into an AC signal. A single-line diagram consisting of PV panels, DC-DC boost converter, and a 3-phase inverter connected to the utility grid through a matching transformer is illustrated in Fig 1. In this model, the PV array is designed to generate a rated power of 100*kW* under standard operating conditions (S = lOOO W/m$^2$ and T = 25°C). The array is connected to the DC-DC boost converter operating with a duty cycle controlled by a Maximum Power Point Tracker (MPPT).

The main advantage of this algorithm is its fast power tracking process but it might be unstable when the solar intensity is low due to the low current differentiation[4]. The MPPT algorithm used in this system is based on the ``Incremental Conductance and Integral Regulator" technique that sets the output voltage for optimal operation. The boost converter is connected to the 3-phase inverter to convert DC into AC. The AC power output of the inverter is synchronized with the grid using a Phase Locked Loop (PLL). In this study, the islanding detection technique is implemented within the PV-based inverter and is designed to de-energize the system[5]

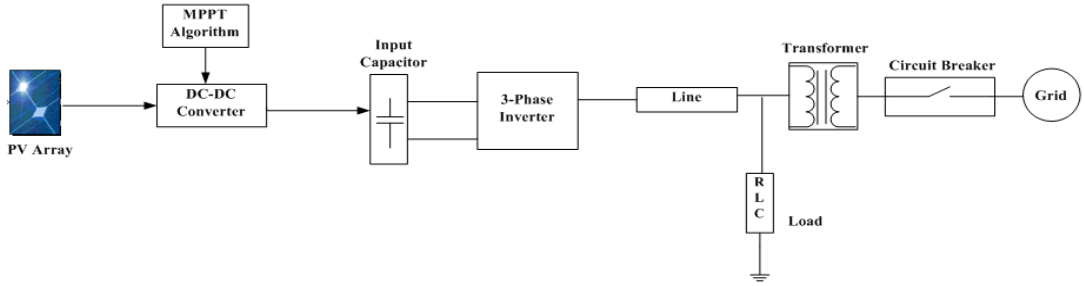


**Fig 1:**Single-line diagram of a grid-connected PV system.

Whenever islanding is detected. A series R-L filter with a capacitor bank is used to filter out the harmonics produced by the high frequency switching in the inverter. At the PCC, the inverter is connected to both the RLC load, The effect of changing the load quality factor ($Q_f$ ) on the detection waveform was also investigated. $Q_f$ is de_ned as the ratio of the reactive power consumption to the rated power output of the DG inverter. IEEE standards require the islanding detection technique to be operational with loads having $1<Q_f<2.5$ at resonant frequency [6].and a step-up transformer which is connected to the main utility. The utility grid is modeled as a 25 kV equivalent transmission system fed by a 120-kV infinite bus. To simulate islanding, a circuit breaker on the utility side is turned to the open position. The MATLAB Simulink model of this grid-connected PV system is depicted in Fig 2.

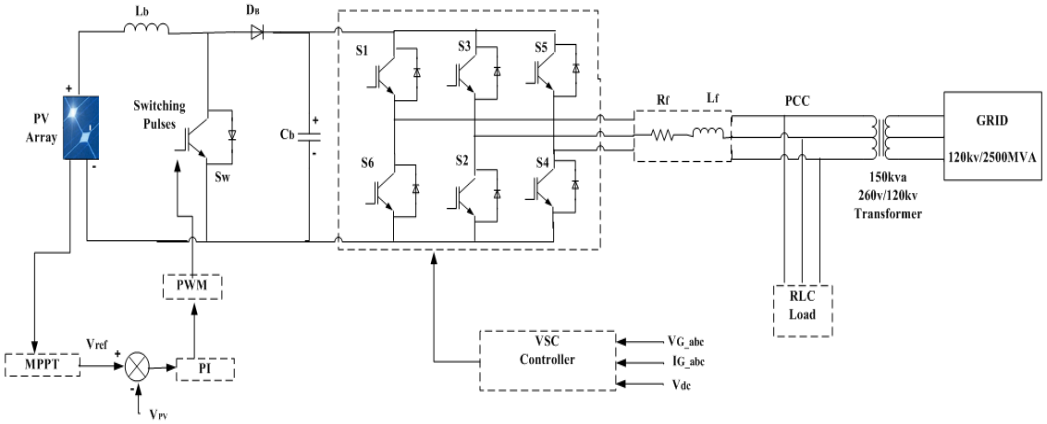


**Fig 2** Block diagram of grid-connected PV system**.**

 2017 IJLERA – All Right Reserved 

The inverter's control system consists of two loops: 1) an external loop controlling the DC link voltage and, 2) an internal loop controlling the active (*Id)* and reactive (*Iq*) orthogonal current components as shown in Fig 3**.** The reference setting for the *Id* component is determined by an external voltage controller while the value of the *Iq* component is set to zero to maintain unity power factor (*PF* =1).The dc-link voltage controller is designed for balancing the power flow in the system. In this paper, a synchronous reference frame control is chosen. It is also called as dq control. It uses a reference frame transformation module, abc to dq to transform the grid current and voltage waveforms into a reference frame that rotates synchronously with the grid voltage so that the control variables become dc values. [7]

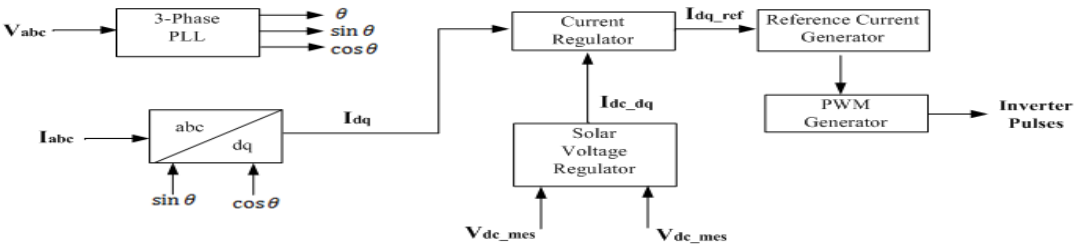


**Fig 3** VSC Controller

Thus, filtering and controlling can be easily achieved; the dc- link voltage is controlled in accordance with the PV output power. Its output acts as reference for the active current controller (Idref), whereas the reference for the reactive current controller (lqref), is set to zero, as the photovoltaic system connected to low voltage distribution network is expected to deliver only active power under normal scenario. Hence, the current vector is always in phase with the grid voltage. The dq control structure is associated with K factor controllers since they have a satisfactory behavior while regulating dc variables. The phase angle used for the abc to dq transformation module is obtained by the Phase-Locked Loop (PLL).

The DC link capacitor acts as energy storage element. The photovoltaic (PV) array output power varies with the atmospheric conditions, such as insolation and temperature. By maintaining the DC link voltage at a constant reference, the inverter supplies power to the AC grid by injecting a current proportional to the PV array output power. The reference DC link voltage, Vdcref is calculated from the following relations[8]

$$V_{an} = m_a \frac{V_{dcref}}{2} \rightarrow V_{dcref} \geq \frac{2}{m_a} V_{an}$$

$V_{an}$ is the peak line to neutral voltage of the grid equal to 204V. $m_a$ Is the amplitude modulation index of the sine triangular PWM, chosen as 0.8. Therefore the $V_{dcref}$ is calculated as 500V.A filter at inverter output terminals is connected to remove high switching frequency components from output current of inverter. The design of LC filter is given in this paper. As the PV array of 100kW is used for integration with 260 V, 50 Hz there phase network, the RMS value of rated fundamental line current, h, in each line is 47 A at standard test conditions (STC) of PV cell (S = lOOO W/m$^2$ and T = 25°C). Hence, the peak value of the line current, IL, is 66.6 A. Assume that the allowed peak ripple current, $I_L$. I ' at switching frequency is ripple 2.5 % of the rated current, which is approximately equal to 1.665A. For $m_a$ = 0.8, the peak inverter output voltage at switching frequency is given below

$$V_a = 0.818 \frac{V_{dc}}{2}$$

$$L = \frac{V_a}{2\pi f_s I_{ripple}}$$

## II. PROPOSED ISLANDING DETECTION TECHNIQUE

A passive islanding detection technique based on monitoring the ripple content in the instantaneous output voltage of the inverter at the PCC using time-domain spectral analysis is developed. Under steady state conditions, the output power of the PV inverter has small variations due to high switching frequencies, dead time, and DC link voltage ripple. These variations are normally absorbed by the grid due to its low impedance and their effect is not observed at the PCC voltage level. The single-phase voltage $V_{island}$ at the PCC level after islanding is mathematically expressed as where $V_{grid}$ is the root mean square (RMS) phase voltage on the utility side of the grid, $P_{inv}$ is the 3-phase inverter output power, and $P_{Load}$ is the power consumed by the load. Since

 2017 IJLERA – All Right Reserved 

$V_{grid}$ and *PLoad* are considered constants, any power variation in $P_{inv}$ is directly reflected in $V_{island}$ . As shown in Fig 4(b), sustained oscillations in $V_{island}$ is observed when islanding occurs and is uniquely different from other disturbances under normal and fault conditions, as illustrated in Fig. 4(a) and 4(c), respectively. [9]

In case of zero power mismatch, the DG source is fully capable of delivering the load demand ($P_{inv}$ = $P_{Load}$ ). In this case, conventional passive techniques will fail to detect islanding, therefore this is considered the worst case scenario in this study. For the 3-phase short-circuit case in Fig. (c), the fault was shown to clear within two cycles while for the islanding case, the voltage flactuations did not diminish but persisted as shown in Fig. 4(b). Based on these observations, the proposed technique is effectively used to detect islanding by monitoring the ripple content in the $V_{island}$ waveform. A block diagram of this technique using Simulink is presented in Fig. 5. The DG source is fully capable of delivering the load demand ($P_{inv}$ = $P_{Load}$ ). In this case, conventional passive techniques will fail to detect islanding, therefore this is considered the worst case scenario in this study. For the 3-phase short-circuit case in Fig. 4(c), the fault was shown to clear within two cycles while for the islanding case, the voltage fluctuations did not diminish but persisted as shown in Fig. 4(b). Based on these observations, the proposed technique is effectively used to detect islanding by monitoring the ripple content in the $Vi_{sland}$ waveform. A block diagram of this technique using Simulink is presented in Fig. 5.

As the ripples in the RMS voltage waveform is first amplified by taking its derivative. The derivative signal is then passed through an RMS block to determine the ripple content of the amplified waveform and eliminate the DC component.

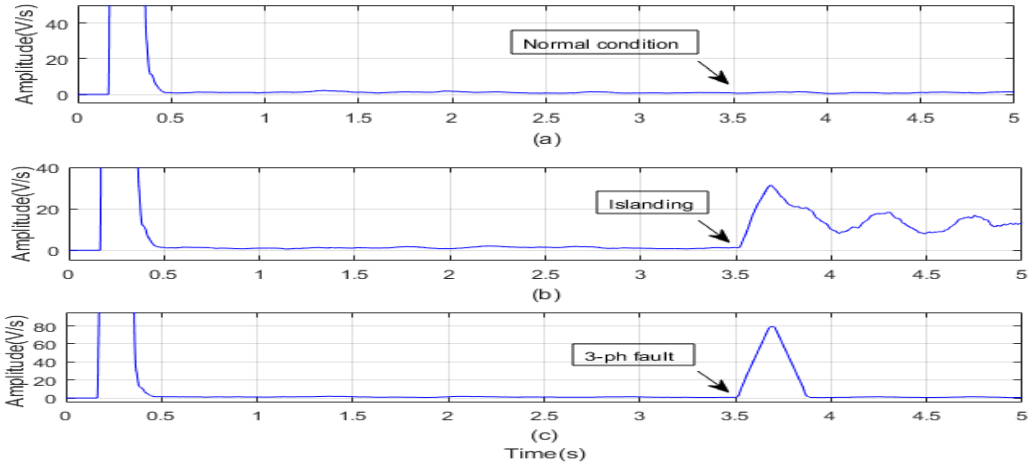


Fig 4. Root mean square (RMS) of single-phase voltage waveforms at PCC. (a) Grid-connected condition. (b) Islanding condition. (c) 3-phase short-circuit fault condition.

Three moving average lowpass filters (`Mean') blocks are used after each output stage. The first mean block eliminates any high frequency noise above 60 Hz in the input RMS voltage, while the second eliminates any points of discontinuity in the output of the derivative block. Finally, the third mean block is used to smooth out the output of the RMS block. Fig. 6 shows the islanding detection waveform output for the three cases.

From Fig. 6, it is clear that there is a sustained difference in the islanding detection waveform before and after islanding. In the fault scenario, although there is a transient spike in the waveform, it settles down relatively fast. Therefore, a threshold was used to differentiate between the grid-connected and islanded waveforms. In addition, a time delay was introduced in the final detection stage to avoid false tripping due to transients caused by non-islanding scenarios such as faults, load-switching, loss of parallel feeder,

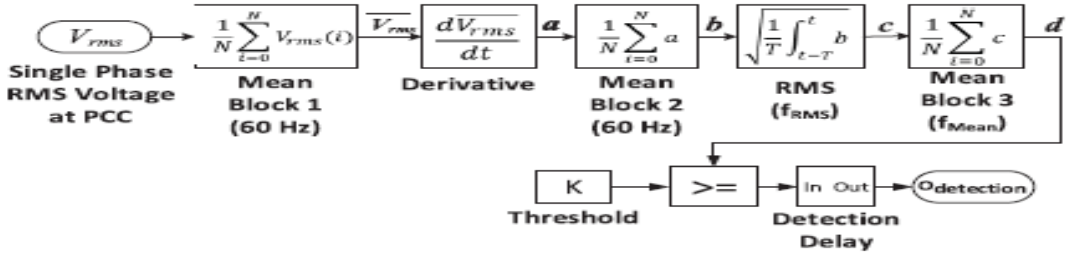


**Fig 5**. Block diagram of the proposed islanding detectiontechnique.

 2017 IJLERA – All Right Reserved 

The ripples in the RMS voltage waveform are first amplified by taking its derivative. The derivative signal is then passed through an RMS block to determine the ripple content of the amplified waveform and eliminate the DC component. Three moving average lowpass filters (`Mean') blocks are used after each output stage. The first mean block eliminates the ripples in the RMS voltage waveform is first amplified by taking its derivative. The derivative signal is then passed through an RMS block to determine the ripple content of the amplified waveform and eliminate the DC component. Three moving average lowpass filters (`Mean') blocks are used after each output stage.

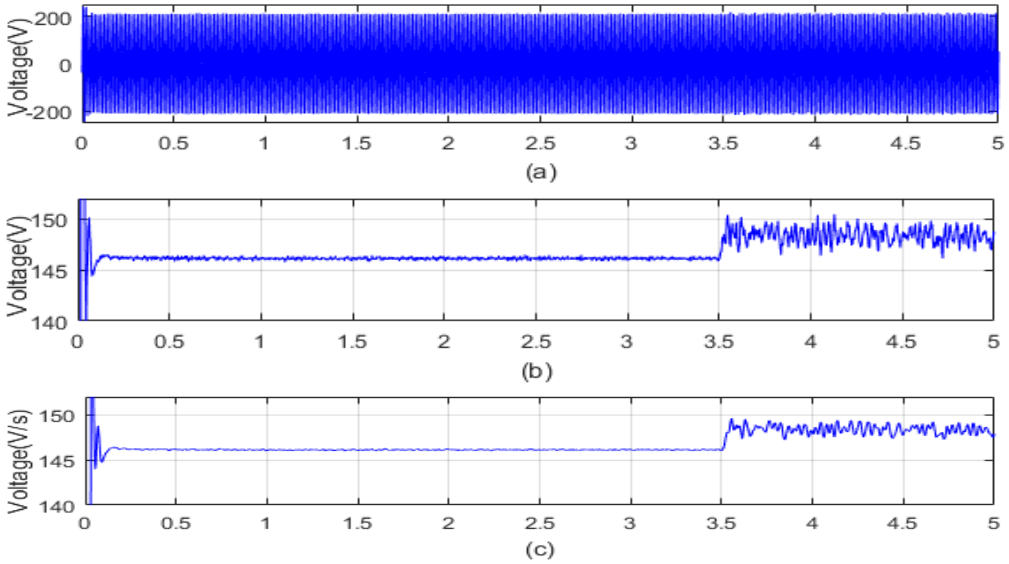


Fig 6. Waveforms of three stages of the islanding detection technique.

## III.a ISLANDING EVENTS

the islanding detection output waveform and the islanding trigger signal, respectively, for an island with zero power mismatch. Before islanding, the waveform stayed well below the predefined threshold. However, after islanding, the Waveform consistently was above the threshold and islanding was detected within 0.3s shown in Fig 7.

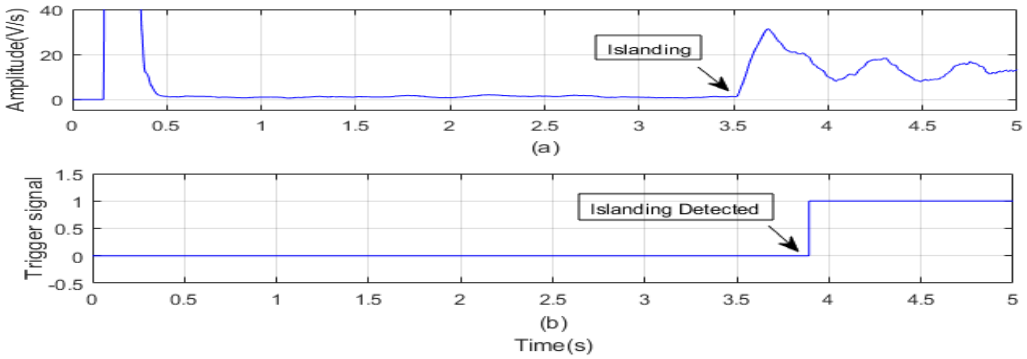


Fig 7.Zero mismatch scenario. (a) Islanding detection waveform. (b) Islanding trigger signal.

## III.b NON-ISLANDING EVENTS

The various possible non-islanding events that can falsely trigger islanding detection are short-circuit faults, loss of a parallel feeder (LOPF), load switching, capacitor switching, non-linear loads, and starting of large motors. Each of these non-islanding scenarios have been simulated to verify the accuracy of the proposed technique.

Fig 8 shows the detection waveforms for several simulated non-islanding events such as short-circuit faults, LOPF, load switching, and capacitor switching. The fault scenarios were simulated by initializing a short-circuit fault on a parallel feeder

 2017 IJLERA – All Right Reserved 

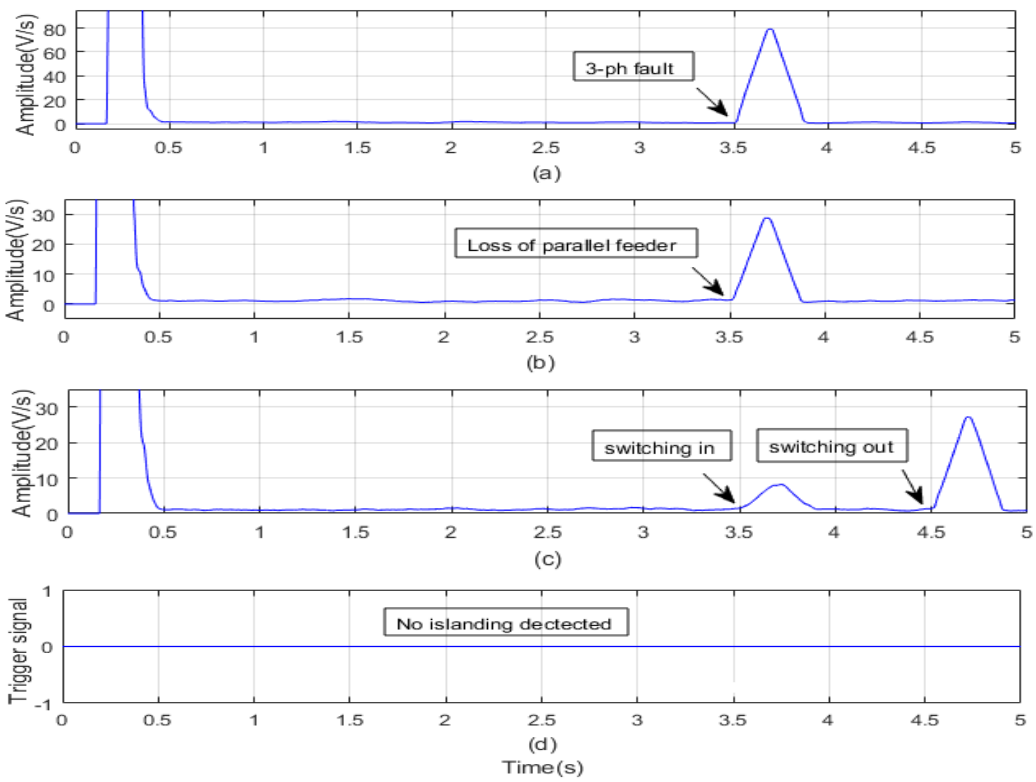


FIGURE 8. (a) 3ph Fault (b) loss of parallel feeder (c) Load switching. (d)Islanding trigger signal.

## CONCLUSION

A passive islanding detection technique for grid connected PV inverters was presented in this paper. The proposed technique monitors, in time domain, the ripple content of the RMS value of the PCC voltage and detects islanding when the ripple content is higher than a predefined threshold for a certain period of time. The proposed technique was thoroughly tested under a variety of possible islanding scenarios.The tested non-islanding scenarios included 3ph-faults, loss of parallel feeder, load switching, The proposed technique successfully detected islanding for all cases including the worst case scenario of zero percent power mismatch. The technique was able to detect islanding within 300ms.Moreover, the technique is computationally inexpensive and can be easily implemented into a PV inverter.

## REFERENCES

[1]. J.a. laghari, h. mokhlis, m. karimi, a.h.a. bakar, hasmaini mohamad Computational Intelligence based techniques for islanding detection of distributed generation in distribution network: A review, 2014 Elsevier Ltd. All rights reserved.

[2]. F. De Mango, M. Liserre, and A. D. Aquila, "Overview of anti-islanding algorithms for PV systems. Part II: Active methods," in *Proc. IEEE Power Electron. Motion Control Conf.*, Aug. 2006, pp. 1884–188.

[3]. Xiaolong Chen and Yongli Li "An Islanding Detection Algorithm for Inverter-Based Distributed Generation Based on Reactive Power Control" *IEEE Transactions On Power Electronics, Vol. 29, No. 9, September 2014.*

[4]. Tey Kok Soon,1 Saad Mekhilef,1 and Azadeh Safari2, "Simple and low cost incremental conductance maximum power point tracking using buck-boost converter" *Journal Of Renewable And Sustainable Energy 5, 023106 (2013).*

[5]. Bikiran Guha Rami J. Haddad Youakim Kalaani," A Novel Passive Islanding Detection Technique for Converter-Based Distributed Generation Systems *©2015 IEEE.*

[6]. John Stevens, Russell Bonn, Jerry Ginn, and Sigifredo Gonzalez "Development and Testing of an Approach to Anti-Islanding in Utility-Interconnected Photovoltaic Systems" *Photovoltaic System Applications Department Sandia National Laboratories.*

 2017 IJLERA – All Right Reserved 

[7]. DivyanagaJakshmi Haribabu, Adithya Vangari,Jayachandra N. Sakamuri."Dynamics of Voltage Source Converter in a Grid Connected Solar Photovoltaic System" Conference Paper · July 2015.

[8]. Ned Mohan, Tore M. Undeland, and William P. Robbins " Power Electronics," 2nd ed. , John Wiley and Son, Inc, 2003.

[9]. Bikiran Guha1 , Rami J. Haddad2 , And Youakim Kalaani2 "Voltage Ripple-Based Passive Islanding Detection Technique for Grid-Connected Photovoltaic Inverters" *IEEE Power and Energy Technology Systems Journal.*

 2017 IJLERA – All Right Reserved 